Calculation of Diffusion-Limited Kinetics for the Reactions in Collision Coupling and Receptor Cross-Linking

Lonnie D. Shea,* Geneva M. Omann,# and Jennifer J. Linderman*
*Department of Chemical Engineering, University of Michigan, and #Department of Surgery and Department of Biological Chemistry, University of Michigan and VA Medical Center, Ann Arbor, Michigan 48109 USA

ABSTRACT Both enzyme (e.g., G-protein) activation via a collision coupling model and the formation of cross-linked receptors by a multivalent ligand involve reactions between two molecules diffusing in the plasma membrane. The diffusion of these molecules is thought to play a critical role in these two early signal transduction events. In reduced dimensions, however, diffusion is not an effective mixing mechanism; consequently, zones in which the concentration of particular molecules (e.g., enzymes, receptors) becomes depleted or enriched may form. To examine the formation of these depletion/accumulation zones and their effect on reaction rates and ultimately the cellular response, Monte Carlo techniques are used to simulate the reaction and diffusion of molecules in the plasma membrane. The effective reaction rate at steady state is determined in terms of the physical properties of the tissue and ligand for both enzyme activation via collision coupling and the generation of cross-linked receptors. The diffusion-limited reaction rate constant is shown to scale with the mean square displacement of a receptor-ligand complex. The rate constants determined in the simulation are compared with other theoretical predictions as well as experimental data.

INTRODUCTION

Signal transduction is initiated by the binding of extracellular ligands to receptors in the plasma membrane. These receptor-ligand complexes then initiate a cascade of reactions that ultimately lead to a cellular response. For some mechanisms, the first step of the cascade involves the interaction of a receptor-ligand complex with another molecule in the plasma membrane. For example, receptor-ligand complexes may act as mobile catalysts for the activation of enzymes in the plasma membrane, a mechanism termed *collision coupling* (Tolkovsky and Levitzki, 1978). This mechanism has been used to describe signal transduction through G-protein coupled receptors (reviewed in Lauffenburger and Linderman, 1993), which are the receptors for many hormones (such as catecholamines and gonadotropins), odorants, and light (reviewed in Neer, 1995; Birnbaumer et al., 1990).

As another example, for ligands with multiple sites, a receptor-ligand complex may interact with an unoccupied receptor. This binding of multiple receptors to a single ligand is termed *receptor cross-linking*. Receptor cross-linking is one mechanism by which receptors aggregate in the plasma membrane. This mechanism has been used to describe viral attachment to cells (Wickham et al., 1990) and the release of histamine from basophils and mast cells (Dembo and Goldstein, 1978; Wofsy et al., 1978; Holowka and Baird, 1992).

Received for publication 24 February 1997 and in final form 16 September 1997.

Address reprint requests to Dr. Jennifer Linderman, Department of Chemical Engineering, University of Michigan, 3074 Herbert H. Dow Building, 2300 Hayward, Ann Arbor, MI 48109. Tel.: 313-763-0679; Fax: 313-763-0459; E-mail: linderma@engin.umich.edu.

0006-3495/97/12/2949/11 $2.00

The kinetics of the reactions that constitute signal transduction determine the cellular response. The objective of this study is to examine the kinetics of both the collision coupling and cross-linking mechanisms in terms of the physical characteristics of the tissue and ligand. Knowledge of the expected effect of the various parameters on the reaction kinetics in conjunction with experimental data can lead to a better understanding of the signal transduction mechanism and, ultimately, strategies to manipulate the signaling pathway.

For reactions between species in the plasma membrane, the diffusivity of the species is thought to affect the reaction rates. Experimental data suggest that the diffusivity of molecules in the plasma membrane affects these reaction rates (Bakardjieva and Helmreich, 1979; Gorospe and Conn, 1987; Hanski et al., 1979; Atlas et al., 1980; Goldstein et al., 1981; Jans, 1992). The relationship between diffusivity and reaction rates has been well studied for soluble ligand binding to cell surface receptors (reviewed in Lauffenburger and Linderman, 1993); however, this relationship is not well understood for the reactions within the plasma membrane. Mathematical models are being developed to examine all aspects of the reaction kinetics, such as the initial rates (Lamb, 1994) and the effects of the species concentration (Saxton and Owicki, 1989). One well-studied mechanism involves the trapping of mobile receptors by coated pits (Adam and Delbruck, 1968; Berg and Purcell, 1977; Keizer, 1985; Goldstein et al., 1988).

Studies of two-dimensional reaction-diffusion systems (e.g., Lindenberg et al., 1994; Fichtorn et al., 1989) suggest that the spatial distribution of molecules plays a critical role in determining the reaction rate. Reactions occurring in two dimensions can produce zones in which the concentration of certain species becomes increased or decreased as compared to the bulk concentration. These depletion/accumulation

zones affect the ability of species to interact and therefore the reaction rates. The formation of these depletion/accumulation zones is related to the mechanism of the reaction. We use the term *spatial effects* to represent the effects that the depletion/accumulation zones have on the effective reaction rate.

In this paper, two signal transduction mechanisms (collision coupling and receptor cross-linking) are examined for the presence of either depletion or accumulation zones. Using Monte Carlo techniques to simulate the reaction and diffusion of species in the plasma membrane, we can observe these depletion/accumulation zones and determine their effects on the effective diffusion-limited rate constant. The physical parameters, such as diffusivity and ligand concentration, are examined for their effect on the depletion/accumulation zone and the reaction rates. To compare reaction rates over a range of diffusivities, a dimensionless reaction rate constant is used, which is given by

$$\alpha = \frac{k}{k_h} \tag{1}$$

where k is the effective diffusion-limited reaction rate constant determined from the simulation, and k_h is the diffusion-limited rate constant if the reacting species are homogeneously distributed. The simulation results will be compared to the theoretical estimates predicted for similar mechanisms.

METHODS

A triangular lattice is used to simulate a section of the plasma membrane. Monte Carlo techniques are used to simulate the reaction and diffusion of the various species in the plasma membrane. Simulations are performed using the procedure described by Mahama and Linderman (1994) and used by Shea and Linderman (1997).

Collision coupling model

Fig. 1 shows the reactions that constitute the collision coupling model. Ligand (L) binds to a receptor (R) with rate constant k_f ($M^{-1}\ s^{-1}$), thus forming a receptor-ligand complex (RL). Ligand dissociates from RL with rate constant k_r (s^{-1}). Reactions between RL and inactive enzymes (E) produce activated enzymes (E*), but leave RL intact. In the simulation, the activation of enzymes occurs after collisions between RL and E. Note that the diffusion-limited activation rate constant k_+ ([no./cell]$^{-1}\ s^{-1}$) shown in Fig. 1 is not a specified input, but rather is determined from the simulation. The activated enzyme is deactivated with rate constant k_i (s^{-1}).

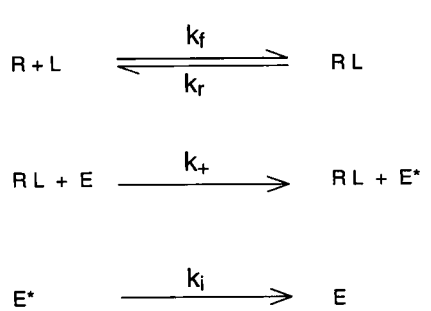

FIGURE 1 Reaction schematic for the collision coupling model. The collision coupling model assumes that the receptor-ligand complex acts as a mobile catalyst for enzyme activation. Simulations are performed to determine the activation rate constant k_+.

The simulations proceed until a steady state is reached. Note that to achieve steady state, no particles (receptors or enzymes) are added to the simulation. Rather, a steady state occurs because of the cyclic nature of the reaction mechanism. At steady state, the number of bound receptors can be calculated by

$$\frac{[RL]}{R_{tot}} = \frac{[L]/K_D}{1 + [L]/K_D} \tag{2}$$

where R_{tot} is the total receptor number, and K_D is the equilibrium dissociation constant for ligand binding to receptor and is equal to

$$K_D = \frac{k_r}{k_f} \tag{3}$$

The quantity $[L]/K_D$ is a dimensionless quantity referred to as the *normalized ligand concentration*. This quantity is often used to compare responses at equivalent fractional receptor occupancies, despite variations in k_r or k_f.

Receptor cross-linking model

Fig. 2 shows a reaction schematic for bivalent ligand binding to monovalent receptor (Fig. 2 *a*) and bivalent receptor (Fig. 2 *b*). For the cross-linking of monovalent receptors, only receptor dimers can form; however, for the cross-linking of bivalent receptors, larger clusters can form. Note that for the bivalent receptor, not all pathways between states are shown in the figure, because of the complexity; however, all possible reactions are allowed in the simulation. For example, there are seven possible cross-linking reactions involving monomers and dimers to form trimers; however, only three of those reactions are shown. A detailed description of the possible reactions and useful notation has been described previously (Dembo and Goldstein, 1978).

Before a cross-link can form, a ligand must first bind to a site on the receptor, which leaves one site available on the ligand. Ligand binds to a receptor with an association rate constant k_f and dissociates from the receptor with rate constant k_r. Note that in Fig. 2 k_f and k_r are defined with respect to a monovalent ligand binding to a monovalent receptor. Cross-links form when a receptor with an empty binding site is adjacent to a receptor-ligand complex in which a ligand has an available binding site. The rate constant for the formation of cross-links is k_x ([no./cell]$^{-1}\ s^{-1}$), and the rate constant for the breaking of a cross-link is

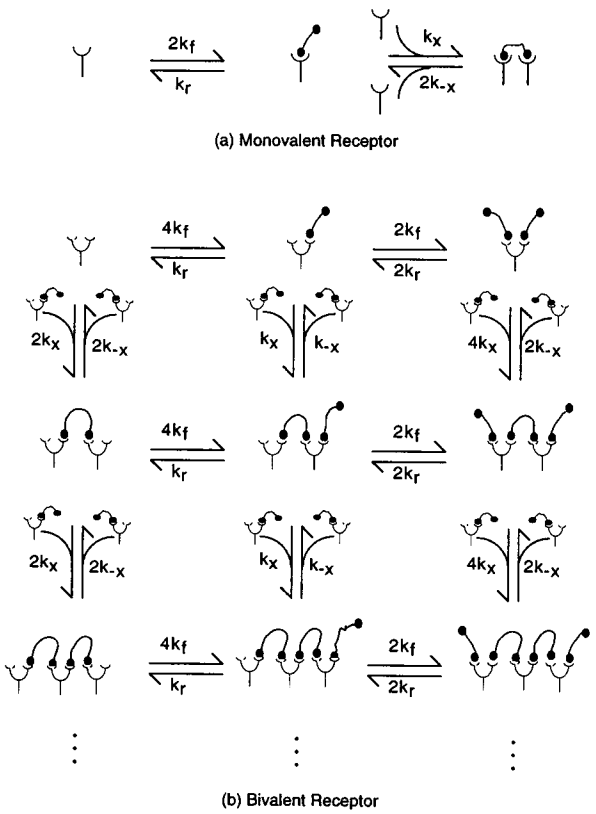

FIGURE 2 Reaction schematic for receptor cross-linking. For the cross-linking of bivalent receptors, not all reactions are shown. Simulations are performed to determine the cross-linking rate constant k_x.

given as k_{-x} (s^{-1}). The diffusion-limited cross-linking rate constant k_x is not an input to the simulation, but is determined from the simulation. Note that k_x and k_{-x} are defined with respect to the cross-linking of monovalent receptors by bivalent ligand. The statistical factors associated with k_f, k_r, k_x, and k_{-x} account for the reaction path degeneracy. As before, the simulations continue until a steady state is achieved; however, no particles are added to achieve a steady state.

A few assumptions have been made regarding the implementation of the cross-linking reactions. We assume that the rate constant for the dissociation of cross-links, k_{-x}, is equal to the ligand dissociation rate constant, k_r, which has been observed experimentally (Subramanian et al., 1996). Next, receptor clusters consisting of more than two receptors are assumed to be immobile. The immobility of large clusters is seen experimentally (Menon et al., 1986), and this assumption does not significantly affect our results. For the diffusion of receptor dimers, the lattice sites to which a receptor can move are only those two that are adjacent to both receptors. Finally, ring formation for all cluster sizes is neglected, which results in the formation of only linear chains. With this latter assumption, we are able to more easily compare simulation results with the model of Dembo and Goldstein (1978), for which the equilibrium cluster size distribution has an analytical solution.

Determination of dimensionless reaction rate constants

To quantify the effects of the depletion/accumulation zones on the reaction rate, we first calculate an effective reaction rate constant at steady state for the reactions in the plasma membrane. These effective rate constants are determined by counting the number of reactions between reacting species in a fixed time interval and then dividing by the average number of reactants in that interval. For the collision coupling model, an effective reaction rate constant (k_+) for the reaction of RL with E is calculated from the simulation by dividing the number of reactions that occur each second by the average number of RL and E for that second. The average number of RL and E for each second is determined by averaging the number of RL and E at the beginning, middle, and end of the interval. For receptor cross-linking, an effective cross-linking rate constant (k_x) is determined by counting the number of cross-linking reactions that occur in an interval and dividing by the average number of reactants. For the cross-linking of bivalent receptors, only the 15 cross-linking reactions involving monomers and dimers are used to determine k_x. These reactions are used because they occur with a relatively high frequency as compared with clusters larger than two. The reaction rate constants determined from the simulation are divided by the appropriate statistical factors (see Fig. 2) to determine the value of k_x.

The dimensionless rate constant, α, defined in Eq. 1, is calculated from the effective rate constant and the homogeneous rate constant. For the collision coupling mechanism, the effective activation rate constant is given by k_+ and is determined from simulations as just described. Because reactions occur after collisions between RL and E, the expression for the homogeneous reaction rate constant, k_h^{cc}, is given by the collision frequency between two homogeneously distributed molecules undergoing a random walk (Torney and McConnell, 1983):

$$k_h^{cc} = \frac{4(D_{RL} + D_E)}{S} \tag{4}$$

where D_{RL} and D_E are the diffusivities of RL and E, respectively, and S is the surface area. An expression for the dimensionless activation rate constant, α^{cc}, is then given by

$$\alpha^{cc} = \frac{k_+}{k_h^{cc}} = \frac{k_+ S}{4(D_{RL} + D_E)} \tag{5}$$

(The related quantity kS/D is a dimensionless quantity known as the second Damköhler number (Janssen and Warmoeskecken, 1987).) In general, note that deviations of α from 1 represent the spatial effects due to an inhomogeneous distribution. Values for α less than 1 correspond to a decreased rate of reaction due to a depletion zone around reactants. Conversely, values for α greater than 1 correspond to enhanced activation rates due to the accumulation of reactants.

For the receptor cross-linking mechanism, the effective cross-linking rate constant, k_x, is determined from the simulation. Because cross-links form between receptors occupying nearest-neighbor sites, the homogeneous cross-linking reaction rate, k_h^{rc}, is given by the nearest-neighbor frequency for a homogeneous distribution. The nearest-neighbor frequency is similar to the collision frequency, with the primary difference being the number of available sites. A first approximation to the nearest-neighbor frequency for a homogeneous distribution is given by the collision frequency multiplied by the number of nearest neighbors; therefore, for six nearest-neighbor sites on a triangular lattice, the nearest-neighbor frequency is given as

$$k_h^{rc} = \frac{24(D_{C1} + D_{C2})}{S} \tag{6}$$

where D_{C1} and D_{C2} are the diffusivities of the two receptor clusters. Therefore, the expression for the dimensionless cross-linking rate constant, α^{rc}, is

$$\alpha^{rc} = \frac{k_x}{k_h^{rc}} = \frac{k_x S}{24(D_{C1} + D_{C2})} \tag{7}$$

Determination of probability density function

Spatial inhomogeneities in the distribution of molecules can be observed by computing a probability density function (PDF) (McQuarrie, 1976). The PDF is the probability of finding a particle as a function of distance from a central particle. For our purposes, the PDF of interest is for reacting species. Therefore, for the collision coupling model, a PDF is generated for the distribution of inactive enzymes (E) around receptor-ligand complexes (RL). For receptor cross-linking, the PDF is generated for receptor-ligand complexes with a free ligand site around a receptor with a free site. To determine the PDF, the number of reactive particles within a 40-site radius of the central particle is counted. Reactive particles that are the same minimum number of jumps from the central particle are grouped together. After counting the number of reactive species, the count at each distance is divided by the number of lattice sites at that distance. To compare PDFs for different simulations, the PDF from the simulation is normalized by the PDF for a homogeneous distribution. Normalized PDFs are determined at steady state for both enzyme activation and receptor cross-linking.

Parameters

A 1000 × 1000 site triangular lattice with a lattice spacing of 7 nm, approximately a protein diameter, is used to simulate a 49-μm^2 section of the plasma membrane. For the collision coupling model, parameters characteristic of G-protein activation through G-protein coupled receptors were used as a basis for the simulations. The receptor density was varied from 10/μm^2 to 40/μm^2, which is within the range seen experimentally (Stickle and Barber, 1989; Sklar, 1986; Post et al., 1995). The density of enzymes was varied from 10/μm^2 to 400/μm^2 (Sklar, 1986; Post et al., 1995); however, simulation results were independent of the total enzyme number. The range of values for the receptor and enzyme density corresponds to an occupancy of 0.1–2.2% of the lattice sites. All species were assumed to have the same diffusivity. The diffusivity was varied from 10^{-11} cm^2 s^{-1} to 10^{-9} cm^2 s^{-1}, the range seen experimentally (Gennis, 1989). The ligand dissociation rate constant, k_r, was varied from 0.1 to 100 s^{-1} (Stickle and Barber, 1991). Values for the inactivation rate constant, k_i, for an activated enzyme were varied from 0.01 to 1.0 s^{-1} (Stickle and Barber, 1991; Taylor, 1990).

For receptor cross-linking, the receptor number was varied from 10 to 100/μm^2, values representative of those seen experimentally (Malveaux et al., 1978; Barsumian et al., 1981). Monomers and dimers were assumed to have the same diffusivity, which was varied between 10^{-11} cm^2 s^{-1} and 10^{-10} cm^2 s^{-1} (Posner et al., 1995; Schlessinger et al., 1976). Several simulations were performed at 10^{-9} cm^2 s^{-1}; however, these simulations were limited because the required computational time for the simulation is large. Values for k_r used in the simulations ranged from 0.2 s^{-1} to 20 s^{-1}. Simulations with values for k_r less than 0.2 s^{-1} were not performed because of the required computational time to reach steady state.

RESULTS

Collision coupling model

Fig. 3 shows the effect of the ligand dissociation rate constant, k_r, and the species diffusivity, D, on the dimensionless activation rate constant for the collision coupling model (α^{cc}). These simulations were performed at a single value of the normalized ligand concentration ($[L]/K_D$) (equal to 0.05) to compare the rate constants for equivalent numbers of receptor-ligand complexes. As k_r is increased

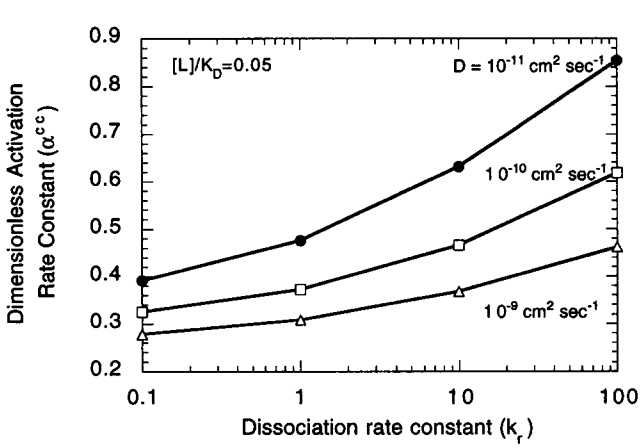

FIGURE 3 The effect of the ligand dissociation rate constant k_r on the dimensionless activation rate constant α^{cc} in the collision coupling model at varying diffusivities. Parameters used in the simulations are $[L]/K_D$ = 0.05, k_i = 0.1 s^{-1}, R_{tot} = 40/μm^2, E_{tot} = 40/μm^2.

from 0.1 s^{-1} to 100 s^{-1}, values of α^{cc} increase. Furthermore, as the diffusivity is decreased from 10^{-9} cm^2 s^{-1} to 10^{-11} cm^2 s^{-1}, values for α^{cc} increase. Values for α^{cc} closer to 1 are indicative of a more homogeneous distribution; therefore, larger values for k_r and smaller values for D correspond to a more homogeneous distribution and decreased spatial effects.

The spatial inhomogeneities produced by the collision coupling mechanism are observed with a probability density function. Fig. 4 *a* shows the effect of varying k_r on the spatial distribution of enzymes around receptor-ligand complexes. Note that as k_r decreases, the size of the depletion zone around a receptor-ligand complex increases. The size of the depletion zone around a receptor-ligand complex controls the steady-state rate constant for enzyme activation. The effect of k_r is attributed to the effect of ligand switching, which is defined as the movement of ligand among receptors (Stickle and Barber, 1989). Although the same number of receptors is bound at steady state for both simulations shown in Fig. 4 *a*, the occupancy is shared differently among the entire receptor population. The equilibrium dissociation constant K_D determines the number of receptors that are bound at equilibrium, and k_r determines the frequency with which the occupancy is redistributed among the receptor population. The movement of ligand among the receptors produces a more homogeneous distribution of enzymes around receptor-ligand complexes, which, by definition, produces values for α^{cc} nearer to unity.

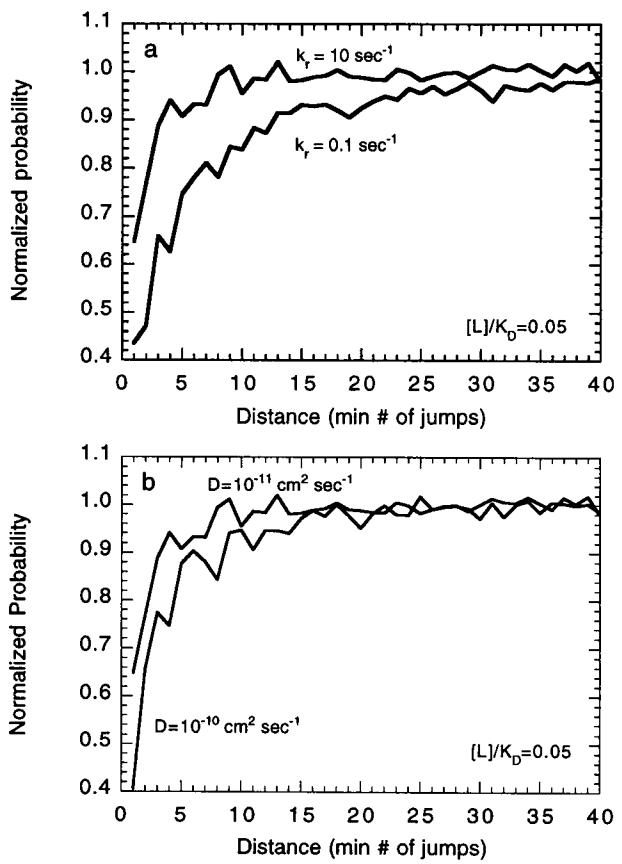

FIGURE 4 Probability density function (PDF) from simulations of the collision coupling model, giving the probability of finding an enzyme as a function of the distance from a receptor-ligand complex. The distance is measured as the minimum number of jumps from a receptor-ligand complex. The PDFs are for (*a*) varying k_r and (*b*) varying D. Parameters used in the simulations are (*a*) $[L]/K_D = 0.05$, $k_r = 1, 10\ s^{-1}$, $k_i = 0.1\ s^{-1}$, $D = 10^{-11}\ cm^2\ s^{-1}$, $R_{tot} = 40/\mu m^2$, $E_{tot} = 40/\mu m^2$. (*b*) $[L]/K_D = 0.05$, $k_r = 1\ s^{-1}$, $k_i = 0.1\ s^{-1}$, $D = 10^{-11}, 10^{-10}\ cm^2\ s^{-1}$ $R_{tot} = 40/\mu m^2$, $E_{tot} = 40/\mu m^2$.

Fig. 4 *b* shows the change in the spatial distribution of enzymes around receptor-ligand complexes produced by varying the diffusivity. Increasing the diffusivity has the effect of increasing the size of the depletion zone and thereby reducing α^{cc}. Receptor-ligand complexes with large diffusivities travel farther on average in a given time than receptor-ligand complexes with small diffusivities. This increased distance of travel enables the receptor-ligand complex with a larger diffusivity to deplete its local environment of inactive enzymes to a greater extent than a receptor-ligand complex with a smaller diffusivity. Thus the enhanced local depletion produced by larger diffusivities produces smaller values for α^{cc}.

The dimensionless activation rate constant for collision coupling, α^{cc}, scales with ratio of the diffusivity (D) to the ligand dissociation rate constant (k_r). The ratio of D/k_r is related to the mean square displacement of a molecule in two dimensions, which is given by (Einstein, 1905)

$$\langle r^2 \rangle = 4Dt \tag{8}$$

where the appropriate diffusivity D to use is the sum of the diffusivities for receptor-ligand complexes and enzymes. The relevant time, t, in Eq. 8 is the mean lifetime of a receptor-ligand complex, which is equal to k_r^{-1}. This effect of the unimolecular lifetime has been observed for a similar reaction mechanism (Keizer, 1982). Fig. 5 shows α^{cc} as a function of the mean square displacement. This scaling of

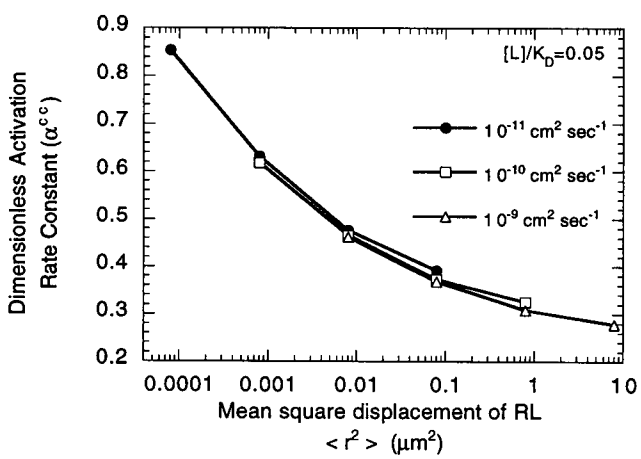

FIGURE 5 Scaling of the dimensionless activation rate constant for the collision coupling model (α^{cc}) as a function of the mean square displacement ($\langle r^2 \rangle$) for a receptor-ligand complex. The data in Fig. 3 are replotted here as a function of $\langle r^2 \rangle$, which is given by Eq. 8.

α^{cc} with the mean square displacement of a receptor-ligand complex is consistent with results for rate constants determined for three-dimensional systems (Keizer, 1983).

The scaling relationship presented above for one normalized ligand concentration can be extended to all normalized ligand concentrations. Fig. 6 shows the dependence of α^{cc} on the ligand concentration at different values of the mean square displacement. In all cases, the trend shown in Fig. 5 holds: an increase in $\langle r^2 \rangle$ means α^{cc} decreases for a constant $[L]/K_D$. At small values of $\langle r^2 \rangle$ and low ligand concentration, the switching of ligand among receptors produces relatively large values for α^{cc} because there are many free receptors for ligand to move among. However, as the normalized ligand concentration increases, the opportunity for switching decreases because of a decrease in the number of unoccupied receptors, and thus values for α^{cc} decrease. At large values of $\langle r^2 \rangle$ and low ligand concentration, the contribution of switching to activation is small and enzyme activation is limited to the vicinity of a few receptor-ligand complexes. As the ligand concentration increases, the increasing number of receptor-ligand complexes produces enzyme activation across the entire cell surface, increasing the activation rate constant. Note that the scaling relationship allows the effects of the normalized ligand concentration ($[L]/K_D$), the diffusivity (D), and the ligand dissociation rate constant (k_r) to be captured in one figure.

Simulations were also performed to determine the effect of the receptor density (R_{tot}), enzyme density (E_{tot}), and the enzyme inactivation rate constant (k_i) on α^{cc} (data not shown). Varying R_{tot}, which affects switching along with the distribution, from 10 to $40/\mu m^2$, affects values for α^{cc} by less than 10%. The effect of the enzyme inactivation rate constant depended on the diffusivity. For a diffusivity equal to 10^{-11} cm^2 s^{-1}, varying k_i from 0.01 to 1.0 s^{-1} affected values for α^{cc} by ~15%. However, for a diffusivity equal to 10^{-10} cm^2 s^{-1}, the same variation in k_i affected α^{cc} by less than 5%. Simulations in which E_{tot} was varied from 10 to $400/\mu m^2$ had no effect on values for α^{cc}.

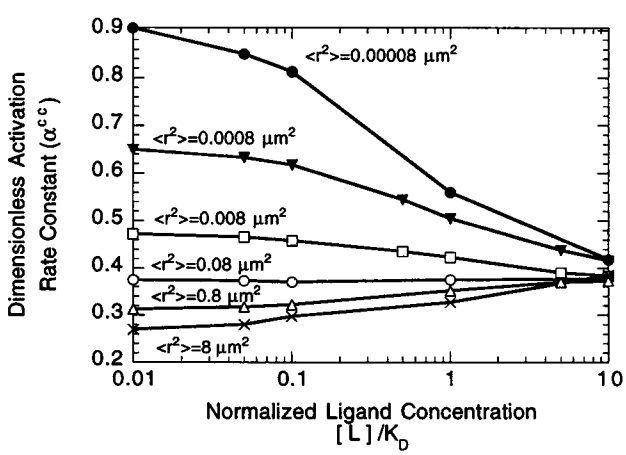

FIGURE 6 Dependence of the dimensionless activation rate constant for collision coupling (α^{cc}) on the normalized ligand concentration at different values of the mean square displacement for a receptor-ligand complex ($\langle r^2 \rangle$). Parameters used in the simulations are $[L]/K_D$ = 0.01–10, k_i = 0.1 s^{-1}, k_r = 0.1, 1, 10, 100 s^{-1}, D = 10^{-11}, 10^{-10} cm^2 s^{-1}, R_{tot} = $40/\mu m^2$, E_{tot} = $40/\mu m^2$.

Receptor cross-linking model

Fig. 7 shows the effect of the ligand dissociation rate constant, k_r, and the species diffusivity, D, on the dimensionless cross-linking rate constant (α^{rc}) for the receptor cross-linking model. These simulations were performed at values of $[L]/K_D$ equal to 0.5 and a receptor density of $10/\mu m^2$. In general, values for the dimensionless cross-linking rate constant α^{rc} are closer to 1 than are the values of the dimensionless activation rate constant for collision coupling α^{cc}. For the cross-linking of monovalent receptor (Fig. 7 *a*), α^{rc} increases with increasing k_r and decreasing D; however, note that the values for α^{rc} are approximately unity for k_r equal to 0.2 s^{-1} and are greater than 1 for larger values of k_r. Values for α^{rc} greater than 1 indicate that there is an accumulation of reactants that increases the overall reaction rate. For the cross-linking of bivalent receptor (Fig. 7 *b*), the spatial effects on the rate constant are smaller than those shown in Fig. 7 *a* when D and k_r are varied. Values for

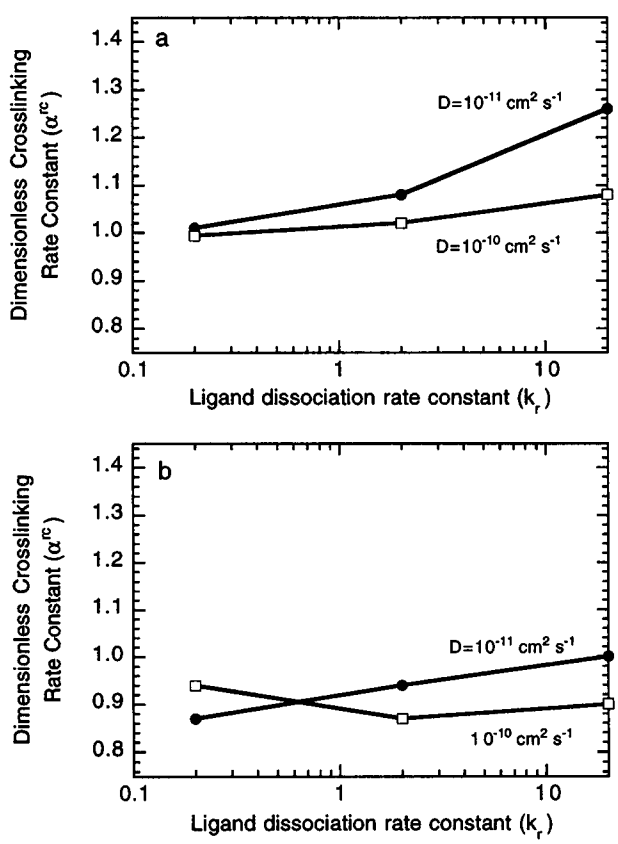

FIGURE 7 The effect of the ligand dissociation rate constant k_r on the dimensionless cross-linking rate constant α^{rc} at varying diffusivities for bivalent ligand binding to (*a*) monovalent receptor and (*b*) bivalent receptor. Parameters used in the simulations are $[L]/K_D$ = 0.5, R_{tot} = $10/\mu m^2$.

α^{rc} vary by less than 15% when D is varied by an order of magnitude and k_r is varied over two orders of magnitude.

Values for α^{rc} near 1 are indicative of a homogeneous distribution, which is observed in the PDF. Fig. 8 shows representative PDFs for the cross-linking of monovalent and bivalent receptors. Note that for the monovalent receptor, the normalized probability is slightly larger than 1 near the central particle, which indicates an accumulation of reacting species. In general, these PDFs are more homogeneous than the PDFs for the collision coupling model. The cross-linking mechanism produces values for α^{rc} near 1 because of the reversibility of the reaction. The breaking of a cross-link can be immediately followed by the formation of the cross-link because the two species are still in the same vicinity.

Similar to the collision coupling mechanism, the dimensionless cross-linking rate constant for the cross-linking of monovalent receptors by bivalent ligand scales with the mean square displacement of a receptor-ligand complex. Fig. 9 shows this scaling relationship for diffusivity and k_r, with each varying over three orders of magnitude. The mean square displacement is related to the size of the accumulation zone, which is related to the ability of two receptors to reform a cross-link once the initial link has been broken.

Simulations examining the effect of the normalized ligand concentration and the receptor density on the dimensionless cross-linking rate constant showed that neither parameter affects the rate constant significantly. Furthermore, the steady-state results of our simulation are consistent with the analytical solution for the formation of linear chains by Dembo and Goldstein (1978). Using the values for k_x determined in the Monte Carlo simulation along with the appropriate values for k_r, the receptor number, and the normalized ligand concentration in the Dembo model, the results of the Monte Carlo simulation can be reproduced.

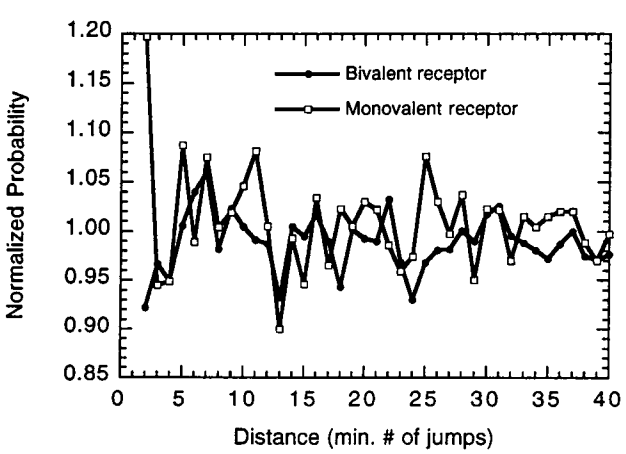

FIGURE 8 Probability density function (PDF) from simulations of receptor cross-linking, giving the probability of finding a free receptor site as a function of the distance from a receptor-ligand complex with a free ligand site. The distance is measured as the minimum number of jumps from the receptor-ligand complex. Parameters used in the simulation are $[L]/K_D$ = 0.5, k_r = 2 s^{-1}, D = 10^{-11} cm^2 s^{-1}, R_{tot} = $10/\mu m^2$.

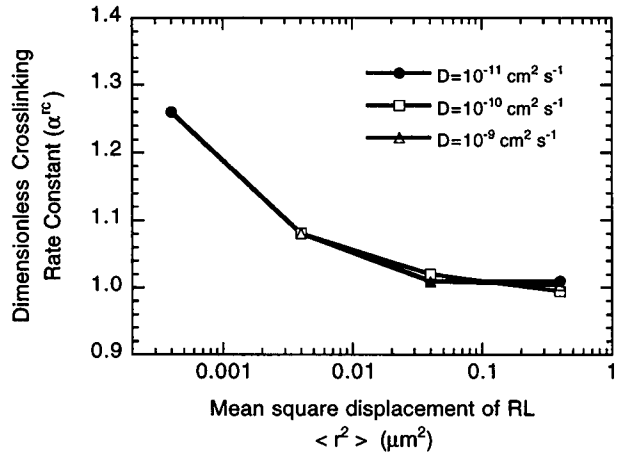

FIGURE 9 Scaling of the dimensionless cross-linking rate constant (α^{rc}) as a function of the mean square displacement ($\langle r^2 \rangle$), at varying D for cross-linking of a monovalent receptor by a bivalent ligand. The parameters used in the simulation are $[L]/K_D$ = 0.5, k_r = 0.02, 0.2, 2, 200 s^{-1}, D = 10^{-11}, 10^{-10}, 10^{-9} cm^2 s^{-1}, R_{tot} = $10/\mu m^2$.

DISCUSSION

The effective plasma membrane reaction rates for two signal transduction mechanisms (collision coupling and receptor cross-linking) were examined to quantify the effects of an accumulation/depletion zone on the reaction rate constant. Monte Carlo techniques were used to simulate these reaction mechanisms and to determine a dimensionless reaction rate constant, α. For the collision coupling mechanism, the irreversibility of the activation reaction results in the formation of a depletion zone around the receptor-ligand complex, which reduces the effective reaction rate below that for a homogeneous distribution ($0.25 \leq \alpha^{cc} \leq 0.9$) for the parameter ranges tested. The size of the depletion zone varies with the diffusivity and ligand dissociation rate constant k_r in such a manner that the dimensionless activation rate constant α^{cc} scales with the mean square displacement of a receptor-ligand complex, as seen in three-dimensional systems (Keizer, 1983). In receptor cross-linking, the reversibility of the mechanism produces a spatial distribution that ranges from a slight depletion zone to a slight accumulation zone. For the cross-linking of monovalent receptors, a small accumulation zone develops around receptor-ligand complexes that enhances the reaction rate above that for a homogeneous distribution ($1 \leq \alpha^{rc} \leq 1.25$) for the parameter ranges tested. Furthermore, the dimensionless rate constant scales with the mean square displacement of a receptor-ligand complex. For the cross-linking of bivalent receptors, a small depletion zone develops around receptor-ligand complexes that reduces the effective reaction rate constant below that of a homogeneous distribution ($0.85 \leq \alpha^{rc} \leq 1$) for the parameter ranges tested.

It is worthwhile to compare results of our Monte Carlo simulations of the collision coupling model with various analytical predictions of the diffusion-limited rate constant, k_+. To better understand the importance of the various

parameters, we compare the dimensionless quantity $k_+S/D_{RL,E}$ from our simulations with that predicted by the various models, where $D_{RL,E}$ is equal to the quantity $D_{RL} + D_E$. For the three models examined, we focus on two aspects of the quantity $k_+S/(D_{RL,E})$: the predicted value and the functional dependence on the various physical characteristics of the system, such as the diffusivity and the unimolecular lifetime.

First we compare the diffusion-limited rate constant from our simulations of the collision coupling model with that predicted for the trapping of receptors by uniformly distributed static sinks. Multiple derivations (Adam and Delbruck, 1968; Berg and Purcell, 1977; Keizer, 1985; Lauffenburger and Linderman, 1993) have been performed that predict a diffusion-limited rate constant with the form

$$\frac{k_+S}{D_{RL,E}} = \frac{2\pi}{\ln b/s - C} \tag{9}$$

where b is the average distance between enzymes, s is the encounter radius, and C is a constant that is dependent on the derivation method. Adam and Delbruck (1968) predict $C = 0.5$; Berg and Purcell (1977), $C = 0.75$; Keizer (1985), $C = 0.231$; Lauffenburger and Linderman (1993), $C = 0$. An estimate for the average distance between enzymes, b, was determined as (Lauffenburger and Linderman, 1993) $b = (S/\pi[E])^{1/2}$, where $[E]$ is the concentration of inactive enzymes. Fig. 10 plots the quantity $k_+S/(D_{RL,E})$ as a function of the diffusivity (Fig. 10 *a*), the ligand dissociation rate constant (k_r, which represents the unimolecular lifetime of the reactant) (Fig. 10 *b*), and the normalized ligand concentration ($[L]/K_D$) (Fig. 10 *c*). Because the various derivations of Eq. 9 differ only slightly, we plot only the Lauffenburger and Linderman solution ($C = 0$). Fig. 10 shows that the quantity $k_+S/(D_{RL,E})$ predicted by Eq. 9 varies slightly with diffusivity (Fig. 10 *a*), is independent of unimolecular lifetime (Fig. 10 *b*), and changes with the normalized ligand concentration (Fig. 10 *c*). The dependence on diffusivity and normalized ligand concentration is indirect and results from changes in b with the changing number of inactive enzymes. Note that this dependence on the number of enzymes differs from what is observed in the simulations. Furthermore, the differences between the values for the rate constant predicted by Eq. 9 and those determined from the simulation can be attributed to the concentration profile, which determines the size of the depletion zone. The assumption of a uniform distribution of traps used to derive Eq. 9 differs from the random distribution of receptors and enzymes in the simulation and may contribute to differences in the concentration profile.

A second comparison can be made to the model by Goldstein et al. (1988) for the trapping of mobile receptors by randomly distributed static traps. Their solution, given in our notation, is

$$\frac{k_+S}{D_{RL,E}} = 2\pi\alpha\gamma\frac{K_1(\gamma a)}{K_0(\gamma a)} \tag{10}$$

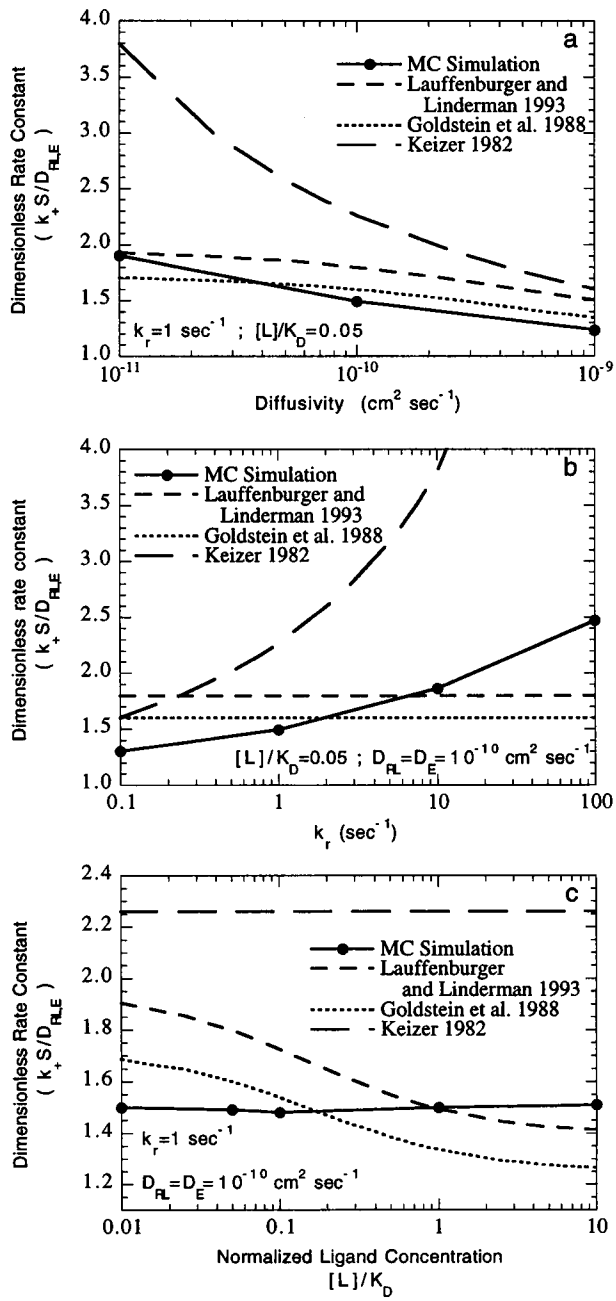

FIGURE 10 Comparison of the dimensionless rate constant $k_+S/(D_{RL} + D_E)$, determined from our Monte Carlo simulations of the collision coupling model with the predictions of Lauffenburger and Linderman (1993), Goldstein et al. (1988), and Keizer (1982). The figures show the functional dependence on (*a*) the diffusivity of each species (e.g., D_{RL}, D_E); (*b*) the ligand dissociation rate constant k_r, which determines the unimolecular lifetime of a receptor-ligand complex; and (*c*) the normalized ligand concentration. Parameters used to generate the curves are $k_i = 0.1\ s^{-1}$, $S = 49\ \mu m^2$, $R_{tot} = 40/\mu m^2$, $E_{tot} = 40/\mu m^2$, $s = a = 3.5$ nm, $R = 7$ nm. For (*a*) $k_r = 1\ s^{-1}$, $[L]/K_D = 0.05$; (*b*) $D_{RL} = D_E = 10^{-10}\ cm^2\ s^{-1}$, $[L]/K_D = 0.05$; and (*c*) $k_r = 1\ s^{-1}$, $D_{RL} = D_E = 10^{-10}\ cm^2\ s^{-1}$.

Equation 10 is based on solving a differential equation for the radial concentration profile and then determining the rate constant based on the flux at the boundary of the trap. In Eq. 10, a is the radius of the trap, K_1 is the modified

Bessel function of the order 1, K_0 is the modified Bessel function of order 0, and γ is given by $(k_+/([E](D_{RL,E})))^2$. Fig. 10 plots the quantity $k_+S/(D_{RL,E})$ as predicted by the model of Goldstein et al. as a function of the diffusivity (Fig. 10 *a*), ligand dissociation rate constant (Fig. 10 *b*), and the normalized ligand concentration (Fig. 10 *c*). The solution by Goldstein et al. is explicitly dependent on the diffusivity, through the parameter γ; is independent of the unimolecular lifetime; and varies with the ligand concentration because of the dependence of γ on $[E]$. Although the simulation and the Goldstein et al. model have similar predictions in Fig. 10 *a*, this is due in part to a fortunate choice of parameters, and agreement cannot be expected for all parameter ranges. For example, increasing the number of inactive enzymes by an order of magnitude had no effect in the simulation, but increases the value predicted by Eq. 10 by 30–50%.

Our final comparison is to a model by Keizer (1982), shown schematically as

$$A + B \xrightarrow{k_+} \text{Products} \tag{11}$$

$$A \xrightarrow{k_r} \text{Products} \tag{12}$$

In a manner analogous to that of the collision coupling model, the rate constant k_r governs the unimolecular lifetime of a reactant. An explicit solution for the diffusion-limited rate constant can be obtained by using nonequilibrium pair correlation functions if the unimolecular lifetime is much shorter than the bimolecular lifetime, i.e., $k_u \gg k_+\rho_A$, $k_+\rho_B$, where ρ_A, ρ_B are the densities of A and B, respectively. For this situation, the diffusion-limited reaction rate constant, in our notation, is given by

$$\frac{k_+S}{D_{RL,E}} = \frac{2\pi}{K_0(R\alpha^{1/2})} \tag{13}$$

where R is the radial distance of closest approach of a receptor-ligand complex and an enzyme, and α is equal to k_r/D_{RL}. Fig. 10 shows the functional dependence of $k_+S/D_{RL,E}$, as predicted by Eq. 13, on the diffusivity (Fig. 10 *a*), the unimolecular lifetime (Fig. 10 *b*), and the normalized ligand concentration (Fig. 10 *c*). Trends similar to the simulation results for diffusivity and the lifetime effect are seen; however, the exact values obtained can differ significantly. Part of the difference can be attributed to the different mechanisms (compare this mechanism with Fig. 1). Another factor that contributes to the different predictions of the simulations and the literature models just discussed, including the Keizer model, is the manner in which a steady state is achieved. In the literature models, the reactions are assumed to be irreversible, and the steady state is achieved by adding reactants to replace those consumed. In contrast, species are not added in our simulations; a steady state is achieved because of the cyclic nature of the mechanism. For example, one reactant is a receptor-ligand complex that is responsible for activating the second reactant, an inactive enzyme. The dissociation of ligand from a receptor essentially removes one reactant, but another reactant can form by ligand binding to a different receptor. In the literature models, the reactants are typically added uniformly; however, the simulations "add" reactants only at specific sites, such as the location of a receptor or an active enzyme. Adding reactants uniformly would mix the system more effectively than addition at discrete locations, thereby producing larger rate constants.

The functional dependence of our predicted activation rate constant for the collision coupling mechanism on the ligand dissociation rate constant is consistent with experimental data. Stickle and Barber (1989, 1991) and Mahama and Linderman (1995) have prevented the movement of ligand among receptors, or switching, by blocking a fraction of receptors with an antagonist and binding the remaining receptors with an agonist. Inhibiting switching reduced the measured response, consistent with a decreased activation rate constant.

Next we compare the rate constants obtained from simulations of receptor cross-linking with values that were determined experimentally. Although the spatial effects on the cross-linking rate constant are less significant than in the collision coupling model, our results offer an interpretation of experimental data that is different from those previously presented. The second column of Table 1 lists the rate constant measured for cross-link formation for IgE dimer on human basophils (Dembo et al., 1982) and a rate constant estimated for DCT_2-cys binding to IgE on cells (Erickson et al., 1991). Using these values, we estimate the dimensionless cross-linking rate constant α^{rc} by using Eq. 7. For cross-linking of IgE on basophils, the reported rate constant is equal to the numerator of Eq. 7. The diffusivity for the Fc_ϵ receptor is $\sim 2 \times 10^{-10}$ cm^2 s^{-1} (Schlessinger et al., 1976). For cross-linking by DCT_2-cys, the reported rate constant is converted to a two-dimensional constant using the cell surface area, the cell density, and Avogadro's number. The two-dimensional rate constant is then made dimensionless by using Eq. 7. The last column of the table lists the dimensionless rate constants for the two experimental cases and the simulations performed here. Comparing the dimen-

TABLE 1 Comparison of the cross-linking rate constants determined experimentally with the diffusion-limited rate constant determined in the simulation

Source	Reported value	Dimensionless rate constant α^{rc}
Dembo et al. (1982)	5×10^{-10} cm^2 s^{-1}	≈0.05*
Erickson et al. (1991)	2.1×10^7 M^{-1} s^{-1}	≈0.0001#
Simulation		≈0.9

*This dimensionless rate constant is obtained by dividing the reported value by $24 \cdot (D_{C1} + D_{C2})$, where $D_{C1} = D_{C2} = 2 \times 10^{-10}$ cm^2 s^{-1}.
#This dimensionless rate constant is determined by multiplying the reported value by $S\rho$ and dividing by $N_{AV} \cdot 24 \cdot (D_{C1} + D_{C2})$, where S is assumed to be 5×10^{-6} cm^2/cell, $\rho = 3.3 \times 10^6$ cells/ml, $N_{AV} = 6.02 \times 10^{23}$ molecules/mol, and $D_{C1} = D_{C2} = 2 \times 10^{-10}$ cm^2 s^{-1}.

sionless rate constants shows that the value of the rate constant from the simulation is significantly larger than values measured or estimated experimentally. Dembo et al. (1982) stated that their measured rate constant was on the order of the diffusion coefficient, and therefore the cross-linking reaction was most likely diffusion-limited. However, according to our simulations, that rate constant is an order of magnitude smaller than the diffusion limit. The measurements by Erickson et al. (1991) are approximately four orders of magnitude less than the values obtained from the simulation and suggest that the cross-linking reaction may not be diffusion-limited. An exact comparison between the literature data and our simulation predictions is complicated by the assumptions associated with the lattice used in the simulations. For example, the triangular lattice assumes six nearest neighbors, which may differ from the physical situation. The formation of cross-links by nearest neighbors assumes a fixed length of the ligand for the cross-link, which can affect the cross-linking rate constant. However, accounting for these phenomena is not expected to alter the simulation results by an order of magnitude or more. Furthermore, because of computational restrictions, the dissociation rate constant for the ligands used in the simulation are greater than those observed by Dembo et al. and Erickson et al. Based on the trends seen in Fig. 7, however, lower values for the dissociation rate constant are not expected to decrease the cross-linking rate constant by an order of magnitude.

To summarize, if the reactions in the plasma membrane are affected by diffusion, the distribution of species in the plasma membrane may not be homogeneous and may significantly affect the reaction rates. Knowledge of how the different parameters, such as diffusivity, ligand dissociation kinetics, and ligand concentration, affect the reaction rate allows a more detailed understanding of the signal transduction mechanism and may provide a significantly different interpretation of experimental data. Modeling studies examining the effects of the physical characteristics of the tissue and ligand used in conjunction with experiments may ultimately lead to strategies for manipulating the signaling pathway and thus the cellular response.

We thank Dr. Robert Ziff for many useful discussions.

This work was supported by an NSF Presidential Young Investigator award to JJL and NSF grant BES-9410403. GMO is supported by the Office of Research and Development, Medical Research Service, Department of Veterans Affairs. Funding was also provided by a NSF graduate fellowship to LDS. Some computing services were provided by the University of Michigan Center for Parallel Computing, which is partially funded by NSF grant CDA-92-14296.

REFERENCES

Adam, G., and M. Delbruck. 1968. Reduction of dimensionality in biological diffusion processes. *In* Structural Chemistry and Molecular Biology. A. Rich and N. Davidson, editors. W. H. Freeman, San Francisco. 198–215.

Atlas, D., D. Volsky, and A. Levitzki. 1980. Lateral mobility of β-receptors involved in adenylate cyclase activation. *Biochim. Biophys. Acta.* 597:64–69.

Bakardjieva, A. G., and E. Helmreich. 1979. Modulation of the β-receptor adenylate cyclase interactions in cultured Chang liver cells by phospholipid enrichment. *Biochemistry.* 18:3016–3023.

Barsumian, E., C. Isersky, M. Petrino, and R. Siraganian. 1981. IgE induced histamine release from rat basophilic leukemia cell lines: isolation of releasing and non-releasing clones. *Eur. J. Immunol.* 11: 317–323.

Berg, H., and E. Purcell. 1977. Physics of chemoreception. *Biophys. J.* 20:193–219.

Birnbaumer, L., J. Abramowitz, and A. Brown. 1990. Receptor-effector coupling by G proteins. *Biochim. Biophys. Acta.* 1031:163–224.

Dembo, M., and B. Goldstein. 1978. Theory of equilibrium binding of symmetric bivalent haptens to cell surface antibody: application to histamine release from basophils. *J. Immunol.* 121:345–353.

Dembo, M., A. Kagey-Sobotka, L. Lichtenstein, and B. Goldstein. 1982. Kinetic analysis of histamine release due to covalently linked IgE dimers. *Mol. Immunol.* 19:421–434.

Einstein, A. 1905. Investigations on the theory of the Brownian movement. *Ann. Physik.* 17:549–560.

Erickson, J., R. Posner, B. Goldstein, D. Holowka, and B. Baird. 1991. Analysis of ligand binding and cross-linking of receptors in solution and on cell surfaces. *In* Biophysical and Biochemical Aspects of Fluorescence Spectroscopy. T. G. Dewey, editor. Plenum Press, New York. 169–195.

Fichtorn, K., E. Gulari, and R. Ziff. 1989. Noise-induced bistability in a Monte Carlo surface-reaction model. *Phys. Rev. Lett.* 63:1527–1530.

Gennis, R. 1989. Biomembranes: Molecular Structure and Function. Springer Verlag, New York.

Goldstein, B., C. Wofsy, and G. Bell. 1981. Interactions of low density lipoprotein receptors with coated pits on human fibroblasts: estimate of the forward rate constant and comparison with the diffusion limit. *Proc. Natl. Acad. Sci. USA.* 78:5695–5698.

Goldstein, B., C. Wofsy, and H. Echavarria-Heras. 1988. Effect of membrane flow on the capture of receptors by coated pits. *Biophys. J.* 53:405–414.

Gorospe, W., and P. Conn. 1987. Membrane fluidity regulates development of gonadotrope desensitization to GnRH. *Mol. Cell. Endocrinol.* 53:131–140.

Hanski, E., G. Rimon, and A. Levitzki. 1979. Adenylate cyclase activation by the β-adrenergic receptors as a diffusion controlled process. *Biochemistry.* 18:846–853.

Holowka, D., and B. Baird. 1992. Antigen-mediated I_GE receptor aggregation and signaling: a window on cell surface structure and dynamics. *Annu. Rev. Immunol.* 8:195–229.

Jans, D. 1992. The mobile receptor hypothesis revisited: a mechanistic role for hormone receptor lateral mobility in signal transduction. *Biochim. Biophys. Acta.* 1113:271–276.

Janssen, L., and M. Warmoeskecken. 1987. Transport Phenomena Data Companion. Edward Arnold Delftse Uitgeuers Maatschappij, London, Baltimore.

Keizer, J. 1982. Nonequilibrium statistical thermodynamics and the effect of diffusion on chemical reaction rates. *J. Phys. Chem.* 86:5052–5067.

Keizer, J. 1983. Trapping by static sinks: an exact result based on fluctuating nonequilibrium thermodynamics. *J. Chem. Phys.* 79:4877–4881.

Keizer, J. 1985. Theory of rapid bimolecular reactions in solution and membranes. *Accounts Chem. Res.* 18:235–241.

Lamb, T. 1994. Stochastic simulation of activation in the G-protein cascade. *Biophys. J.* 67:1439–1454.

Lauffenburger, D., and J. Linderman. 1993. Receptors: Models for Binding, Trafficking, and Signaling. Oxford University Press, New York.

Lindenberg, K., P. Argyrakis, and R. Kopelman. 1994. Diffusion-limited binary reactions: the heirarchy of nonclassical regimes for correlated initial conditions. *J. Phys. Chem.* 98:3389–3397.

Mahama, P., and J. Linderman. 1994. A Monte Carlo study of the dynamics of G protein activation. *Biophys. J.* 67:1345–1357.

Mahama, P., and J. Linderman. 1995. Monte Carlo simulations of membrane signal transduction events: effect of receptor blockers on G-protein activation. *Ann. Biomed. Eng.* 23:299–307.

Malveaux, F., M. Conroy, N. Adkinson, and L. Lichtenstein. 1978. IgE receptors on human basophils: relationship to serum IgE concentration. *J. Clin. Invest.* 62:176–181.

McQuarrie, D. 1976. Statistical Mechanics. Harper and Row, New York.

Menon, A., D. Holowka, W. Webb, and B. Baird. 1986. Cross-linking of receptor-bound IgE to aggregates larger than dimers leads to rapid immobilization. *J. Cell Biol.* 102:541–550.

Neer, E. 1995. Heterotrimeric G proteins: organizers of transmembrane signals. *Cell.* 80:249–257.

Posner, R., K. Subramanian, B. Goldstein, J. Thomas, T. Feder, D. Holowka, and B. Baird. 1995. Simultaneous cross-linking by two nontriggering bivalent ligands causes synergistic signaling of IgE FcεRI complexes. *J. Immunol.* 155:3601–3609.

Post, S., R. Hilal-Dandan, K. Urasawa, L. Brunton, and P. Insel. 1995. Quantification of signalling components and amplification in the β-adrenergic-receptor-adenylate cyclase pathway in isolated adult rat ventricular myocytes. *Biochem. J.* 311:75–80.

Saxton, M., and J. Owicki. 1989. Concentration effects on reactions in membranes: rhodopsin and transducin. *Biochim. Biophys. Acta.* 979: 27–34.

Schlessinger, F., W. Webb, E. Elson, and H. Metzger. 1976. Lateral motion and valence of $F_{c\epsilon}$ on rat peritoneal mast cells. *Nature.* 264:550–552.

Shea, L., and J. Linderman. 1997. Mechanistic model of G-protein signal transduction: determinants of efficacy and effect of precoupled receptors. *Biochem. Pharmacol.* 53:519–530.

Sklar, L. 1986. Ligand-receptor dynamics and signal amplification in the neutrophil. *Adv. Immunol.* 39:95–143.

Stickle, D., and R. Barber. 1989. Evidence for the role of epinephrine binding frequency in activation of adenylate cyclase. *Mol. Pharmacol.* 36:437–445.

Stickle, D., and R. Barber. 1991. Comparisons of the combined contributions of agonist binding frequency and intrinsic efficiency to receptor-mediated activation of adenylate cyclase. *Mol. Pharmacol.* 40:276–288.

Subramanian, K., D. Holowka, B. Baird, and B. Goldstein. 1996. The Fc segment of IgE influences the kinetics of dissociation of a symmetrical bivalent ligand from cyclic dimeric complexes. *Biochemistry.* 35: 5518–5527.

Taylor, C. 1990. The role of G proteins in transmembrane signalling. *Biochem. J.* 272:1–13.

Tolkovsky, A., and A. Levitzki. 1978. Mode of coupling between the β-adrenergic receptor and adenylate cyclase in turkey erythrocytes. *Biochemistry.* 17:3795–3810.

Torney, D., and H. McConnell. 1983. Diffusion-limited reaction rate theory for two-dimensional systems. *Proc. R. Soc. Lond. A.* 387: 147–170.

Wickham, T., R. Granados, H. Wood, D. Hammer, and M. Shuler. 1990. General analysis of receptor-mediated viral attachment to cell surfaces. *Biophys. J.* 58:1501–1516.

Wofsy, C., B. Goldstein, and M. Dembo. 1978. Theory of equilibrium binding of asymmetric bivalent haptens to cell surface antibody: application to histamine release from basophils. *J. Immunol.* 121:593–601.